# Disordered structure of cubic iron silicide films on Si(111)

K. L. Whiteaker, I. K. Robinson, and C. Benson
*Department of Physics, University of Illinois at Urbana-Champaign, Urbana, Illinois 61801*

D. M. Smilgies
*Department of Chemistry, Rutgers University, Piscataway, New Jersey 08855*

N. Onda and H. von Känel
*Laboratorium für Festkörperphysik, Eidgenössische Technische Hochschule Zürich, 8093 Zürich, Switzerland*
(Received 14 September 1994; revised manuscript received 27 December 1994)

X-ray diffraction has been used to analyze a series of thin-film samples of $Fe_xSi$ as a function of thickness and the composition variable $x$. Unannealed samples are found to be composed entirely of a CsCl-type structure not present in the bulk phase diagram. A careful crystallographic analysis is used to show that the variable composition is accommodated by vacancies on the Fe sites. The unit cells of the film are nearly lattice matched to the substrate, which results in a rhombohedral distortion; this lateral strain is compressive for samples near the FeSi composition and tensile for samples near the $Fe_{0.5}Si$ composition. Films annealed to 630 °C are also lattice matched to the substrate but composed of the $\alpha$-$FeSi_2$ structure.

## I. INTRODUCTION

Iron silicide has recently received increased attention (as with other silicides) as possible materials for advancing today's silicon-based semiconductor industry. The specific interest in iron silicide arises because of the presence of a band gap in the bulk phase $\beta$-$FeSi_2$.[1] This has the promise of being a suitable material for the development of a silicon-based electro-optical device. The $\beta$ phase, however, is unlike the cubic $NiSi_2$ or $CoSi_2$, which are metallic and have been successfully grown epitaxially on Si; $\beta$-$FeSi_2$ has a more complex orthorhombic structure that is believed to be due to a lattice instability, which explains the band gap in its electronic structure.[2] In the effort to grow epitaxial iron silicide on Si, pseudomorphic phases have been discovered, which are not seen in the bulk. Technically, these are not true thermodynamic phases, but are stabilized by the substrate and growth conditions. One such pseudomorphic phase is an iron disilicide, with the fluorite structure, called $\gamma$-$FeSi_2$ (Ref. 3) analogous to the $NiSi_2$ and $CoSi_2$ that also have this structure. Another pseudomorphic phase is a CsCl-type structured silicide, which is characteristic of lower growth temperature.[4,5] Recently, we proposed that this phase is best described as $Fe_x\square_{1-x}Si$ with a CsCl-type crystal structure where $\square$ represents iron vacancies.[6,7] The experiments we report have elaborated on the properties of this phase. A series of silicide samples with varying thickness and composition was studied with x-ray diffraction and a discussion of their structure will be presented.

The most common bulk phase of cobalt and nickel silicide is the disilicide, $CoSi_2$ or $NiSi_2$, which has the fluorite ($CaF_2$) crystal structure illustrated in Fig. 1(c). The bulk iron-silicide phase diagram is more complex with a variety of phases; including the orthorhombic $\beta$ phase mentioned above, the cubic $\varepsilon$-FeSi that has a distorted NaCl crystal structure, and the high-temperature tetragonal $\alpha$-$FeSi_2$. The cubic $FeSi_2$ fluorite structure (known as the $\gamma$ phase) and the CsCl phase do not exist in the bulk,[8] but only in epitaxial films. The strain induced by epitaxial growth in thin films is a well-known means of favoring a new structural phase over bulk phases, especially when the favored structure is closely lattice matched to the substrate [an example is bcc Co on GaAs (Ref. 9)]. This is the case for $\gamma$-$FeSi_2$, which has a lattice parameter closely matched with Si and is one of the phases observed

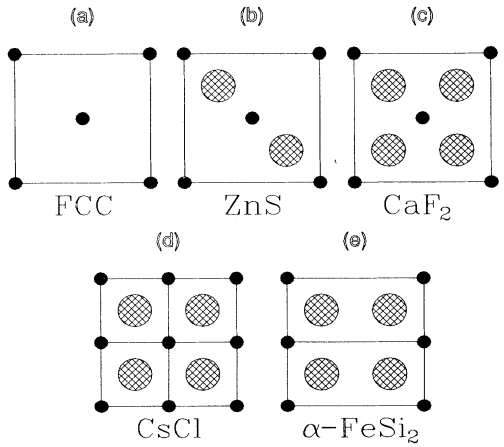


FIG. 1. Comparison of related cubic structures. Each shows the direct cube face made of type-$A$ (metal) atoms as the solid spheres, and a second layer of type-$B$ atoms as larger spheres. The structures are (a) face-centered cubic, (b) zinc blende, (c) fluorite, (d) cesium chloride, and (e) $\alpha$-$FeSi_2$.

 

only in thin films.[3] The case is similar for the $\alpha$-$FeSi_2$, which forms epitaxially far below its bulk formation temperature[10,11] which we also observe.

When $FeSi_y$ is grown by molecular-beam epitaxy (MBE) at room temperature, it does not have the fluorite structure but has the CsCl structure instead. These crystal structures are in fact closely related, as Fig. 1 attempts to demonstrate. The figure shows a series of cubic structures viewed directly on the cube face. It starts with the primitive face-centered-cubic (fcc) lattice made up entirely of atoms of type $A$ in Fig. 1(a). By adding a second kind of atom (type $B$) at four of the $(\frac{1}{4}, \frac{1}{4}, \frac{1}{4})$ positions, this becomes the zinc-blende (ZnS) structure shown in Fig. 1(b). By filling the remaining four $(\frac{1}{4}, \frac{1}{4}, \frac{1}{4})$ positions with $B$ atoms, it becomes the fluorite ($CaF_2$) structure shown in Fig. 1(c). Finally, upon filling the previously empty eightfold coordinates sites between the $B$ atoms with $A$ atoms, this transforms into the CsCl structure [Fig. 1(d)] with a unit cell of half the size. From the point of view of diffraction, structures 1(a)–1(c) all have fcc selection rules, but structure 1(d) is simple cubic; it can be distinguished by the presence or absence of fcc reflections. Structures 1(a)–1(c) can only be distinguished by the relative intensities of their reflections, i.e., by crystallographic analysis. Shown in Fig. 1(e) and discussed in Ref. 12 is the $\alpha$-$FeSi_2$ structure that is also related by removing alternating (100) planes of Fe (type-$A$ atoms) within the CsCl structure.

One reason for drawing the structures beside each other in Fig. 1 is to illustrate the role of disorder. If the $B$ (fluorine) sites in the $CaF_2$ structure are only partially occupied, its diffraction intensities will tend towards the ZnS structure; in the special case of 50% occupation (randomly distributed), we would have the situation of identical stoichiometry and the only distinction between the structures would be small differences in the relative diffraction intensities. The situation for structures 1(c) and 1(d) is analogous. Random 50% occupation of the $A$ sites of the CsCl structure in 1(d) yields a disordered version of the $CaF_2$ structure in 1(c), which, since it has identical stoichiometry, can only be distinguished crystallographically. We report here that this random occupation description represents the case of $FeSi_y$ (or more appropriately $Fe_xSi$) films grown at room temperature on Si(111).

## II. METHOD

The various iron-silicide samples were grown by room temperature MBE. All samples started on cleaned Si(111) surfaces showing a $7\times7$ reconstructure. Samples were grown with a range of thicknesses and with two ratios of stoichiometry. Three silicide films were grown by codeposition of Fe and Si in the ratio of 1:1 after initial deposition of 2 ML of pure Fe. Another set of four samples was grown in a two-step process: the 1:1 codeposition of a template was stopped after 5 Å of growth and the film annealed to 400–500 °C, then additional Fe and Si in a ratio of 1:1 were deposited at room temperature to the desired final thickness. We know from previous x-ray photoemission spectroscopy (XPS) and ultraviolet photoemission spectroscopy (UPS) studies that this annealing step results in a template of cubic $Fe_xSi$.[4] Using this template, five more samples were grown with a Fe to Si ratio of 1:2. Three of these five were overgrown with Si and later annealed to 630 °C. A quartz-crystal monitor was used in each case to determine the film thickness. All unannealed samples were sealed with an amorphous Si cap layer about 20–100 Å thick to protect them during transport through air. For the three annealed 1:2 growth samples, the diffraction scans confirmed the Si cap layers to be epitaxial. A more detailed description of the sample growth can be found in Ref. 13.

The x-ray diffraction experiments were carried out on beamline X16B at the National Synchrotron Light Source at Brookhaven National Laboratory. The fixed geometry of the beamline provides a focused monochromatic x-ray beam with a wavelength of 1.69 Å. The samples were mounted on a Huber four-circle diffractometer and the diffraction intensities measured with a scintillation detector. Both the incident and reflected x-ray beams were defined by $1\times1$-mm$^2$ slits. The Bragg peaks (111), (113), and (220) of the silicon substrate were used to align the substrate to the diffractometer.

Diffraction from the films was measured by means of direct rod scans selecting the measurement points along straight lines in reciprocal space perpendicular to the sample surface. At selected points, integrated intensities were measured by means of rocking curves ($\omega$ scans), performing a background subtraction, and applying corrections for sample area and Lorentz factor. In this paper, the results from the diffraction experiments are organized into four sections: the epitaxial crystal symmetry, the structure factors (or integrated intensities), the film strain, and finally the thickness and uniformity of the silicide films.

## III. CRYSTAL SYMMETRY OF THE FILMS

We used searches for the points of maximum intensity to determine the locations of film Bragg peaks. This differentiated two groups of samples: the unannealed films with differing stoichiometries, and the 1:2 stoichiometry silicide films annealed to 630 °C.

For the unannealed films, the locations of the film Bragg peaks determined the lattice symmetry to be rhombohedrally strained cubic, with the strain axis perpendicular to the interface. The reflections will be indexed in this paper as simple cubic. However, not all the Bragg reflections at fcc positions were seen, which immediately rules out the $CaF_2$ structure found in other silicides such as $NiSi_2$ and $CoSi_2$. So, although the sets of unannealed films were grown with differing stoichiometries, each silicide film has a simple cubic symmetry with a lattice parameter about half that of substrate, implying the CsCl structure for the reasons stated above. Scans in momentum transfer parallel to the (111) interface ($q_\parallel$) through the film Bragg peaks determined the quality of the single crystal epitaxy to the substrate crystal Si(111). The film Bragg reflections were found to be commensurate with the substrate reflections, meaning each film's lattice con-

stant parallel to the epitaxial interface is matched to the corresponding substrate lattice constant. Because of the (111) orientation, the Si substrate projection onto the interface is a two-dimensional hexagonal lattice, which is matched to that of the films. The orientation of the unannealed silicide films to the substrate is $[111]_{\text{film}} \| [111]_{\text{Si}}$ and $[2\bar{1}\,\bar{1}]_{\text{film}} \| [11\bar{2}]_{\text{Si}}$. The film lattice is not a simple continuation of the substrate, but rotated by 180° along an axis parallel to (111); such a rotation is allowed by the hexagonal symmetry of the interface and is usually called *B* type.

These crystal-symmetry results were essentially the same for all the unannealed samples (i.e., all stoichiometries), except to the extent that the strains were different (see below). Because of the *B*-type orientation, the missing peaks were located in relatively empty regions of reciprocal space, so an upper limit of 0.05 can be placed on the fraction of any ordered fluorite phase that might have occurred.

In contrast for the annealed films, Bragg peaks besides the simple cubic reflection were observed at half-order positions along the three (100) directions. As described in Ref. 10, the tetragonal unit cell of the $\alpha$-$FeSi_2$ with three rotational domains provided a (112) plane and pseudohexagonal interface symmetry that is consistent with the observed Bragg reflections. The pseudohexagonal symmetry results from the $c/a$ ratio being 1.9, instead of 2.0 [see Fig. 1(e)] and, thus, the additional half-order peaks. $q_{\|}$ scans through the Bragg peaks determined the film domains to be commensurate with the substrate giving an epitaxy orientation of $(112)_{\alpha} \| (111)_{\text{Si}}$. The films were also strained along this axis perpendicular to the interface.

## IV. STRUCTURE FACTORS

An immediate problem is presented to us in the fact that a range of unannealed samples, with stoichiometries varying by a factor of 2, shows the same CsCl crystal symmetry. As explained in the introduction, this can be due to systematic disorder in the lattice and quantitative (crystallographic) analysis is needed to measure the behavior.

One sample from each of the 1:1 and 1:2 stoichiometric sets was chosen for crystallographic analysis. To obtain the integrated intensity of a reflection, the sample angle $\theta$ was scanned with the detector's aperture set wide open ($10 \times 10$ mm$^2$). For each sample, all Bragg reflections up to the diffractometer limit of 5.6 Å$^{-1}$ were measured. Taking the square root of the integrated intensities gives the structure factor for the scattering of a unit cell, to within an overall scale factor for each sample. Symmetry equivalent reflections were combined into an average structure factor for each data set. Figures 2 and 3 display the measured structure factor versus total momentum transfer. Each reflection is labeled in the cubic representation of the silicide. Note that these are pseudocubic labels, because the strain actually removes some of the symmetry, as can be seen by the different momentum transfer of the two reflections marked (111) and (11$\bar{1}$).

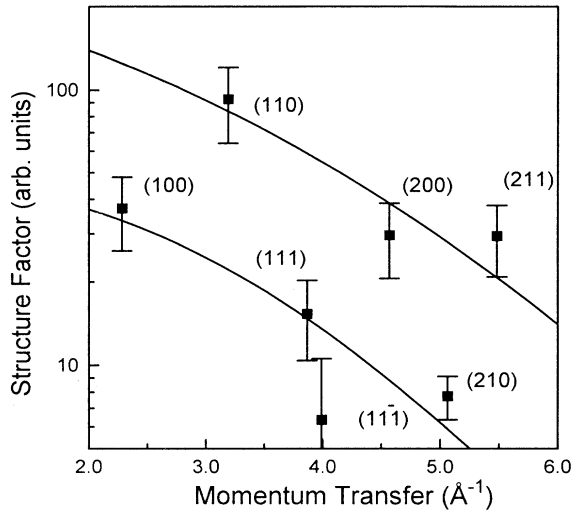


FIG. 2. Structure factors vs total momentum transfer for 1:1 stoichiometric sample, No. 7001. Measured reflections are labeled in the silicide's (strained) cubic coordinates. The top and bottom curve are fits for the CsCl model formulas $F_+$ and $F_-$, respectively, with Fe occupation $x = 0.88$, and Debye-Waller factor 0.33 Å.

The (111) reflection is normal to the surface of the silicide film while there are three inequivalent reflections (11$\bar{1}$), (1$\bar{1}$1), and ($\bar{1}$11), which are more parallel to the surface.

In each case, the general trend of the structure factors divides them into two groups of reflections according to the selection rules of the cubic CsCl atomic structure of Fig. 1(d). This structure is similar to a bcc lattice except the corner and center sites are occupied by different

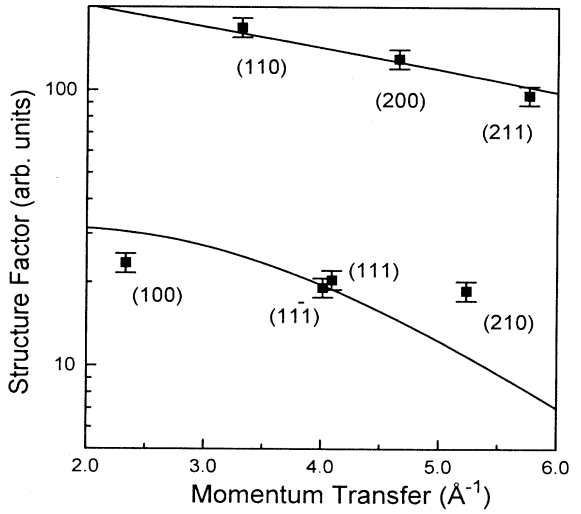


FIG. 3. Structure factors vs total momentum transfer for 1:2 stoichiometric sample, No. 1023. Measured reflections are labeled in the silicide's (strained) cubic coordinates. The top and bottom curve are fits for the CsCl model formulas $F_+$ and $F_-$, respectively, with Fe occupation $x = 0.69$, and Debye-Waller factor 0.10 Å.

atoms. Therefore, the larger structure factors correspond to bcc-allowed reflections with all the atoms scattering in phase. The smaller reflections are due to out-of-phase scattering of the different atoms. In a bcc lattice these latter reflections are absent, but in the CsCl structure the different atomic scattering factors of the Cs and Cl (or Fe and Si) results in a nonzero structure factor. These relative magnitudes of the in-phase and out-of-phase reflections for the two samples are not the same.

To understand why two samples grown with different stoichiometries have the same symmetry, a simple model is constructed for comparison with the observed structure factors. This model is the FeSi in the CsCl structure with a stoichiometry dependence modeled by corresponding occupation of the Fe sublattice, i.e., $Fe_xSi$. Only two different formulas for the structure factors are needed as a function of the momentum transfer. The model structure factor for the bcc type or in-phase reflections is

$$F_+ = A(xf_{\mathrm{Fe}} + f_{\mathrm{Si}})e^{-q^2\langle u^2\rangle/2}$$

and for the bcc absent or out-of-phase reflections it is

$$F_- = A(xf_{\mathrm{Fe}} - f_{\mathrm{Si}})e^{-q^2\langle u^2\rangle/2}.$$

To fit the model to the measured structure factors, three parameters are varied: $x$, the occupation fraction for Fe atoms; $\langle u^2\rangle^{1/2}$, the Debye-Waller rms vibration amplitude for both atoms; and $A$, an overall scale factor that was not removed from the data. The atomic scattering factors for Si and Fe are accurately known, including a dispersion correction for Fe. The dispersion correction is needed because the fixed x-ray energy of 7.1 keV at beamline X16B is close (0.4 keV) to the iron $K$-shell absorption edge.

The curves in Figs. 2 and 3 are the least-squares fit for the model above. On a logarithmic plot, the scale and Debye-Waller factors are represented as an overall displacement and a parabola, respectively, to the fitted curves. The Debye-Waller parameters $\langle u^2\rangle^{1/2}$ for the 1:1 and 1:2 ratio films are $0.33\pm0.10$ and $0.10\pm0.05$ Å, respectively, which compares with 0.075 Å for bulk Si (Ref. 14) and 0.10 Å for bulk Fe.[15] The larger Debye-Waller factor for the 1:1 grown film is believed to be related to its large strain and possibly larger lattice disorder. A noticeable difference between the two samples is the ratio (or difference on the log plot) between the in-phase and the out-of-phase structure factors. The spacing between the two curves is accounted for by the occupation parameter $x$ for iron. For the 1:1 stoichiometry (Fig. 2), the best-fit value is $x=0.88\pm0.13$, near the ideal FeSi(CsCl) structure. For the 1:2 stoichiometry (Fig. 3), the best-fit value is $x=0.69\pm0.08$. This corresponds to a defect CsCl or $Fe_x\square_{1-x}Si$ structure with $\square$ representing statistically random iron vacancies. From the stoichiometry of growth conditions, one would expect the value of $x=1.0$ and $x=0.5$, respectively. The structure-factor data clearly shows a substantial vacancy presence in the CsCl structure. A possible explanation of the discrepancy to the expected values is a relationship to the film strain, which will be discussed below.

We note that the model does not consider the substitution of Fe sites by Si atoms, which could produce similar results, but is considered unlikely because such body-centered Si atoms would need eight nearest-neighbor bonds to the surrounding Si atoms. The strain measurements below also reject this hypothesis.

## V. STRAIN

For strain and film thickness information, scans of the momentum transfer perpendicular to the film $q_\perp$ were performed. We used index scans following the x-ray scattering intensity between the Si substrate Bragg peaks along the lines perpendicular to the surface. These scans measure contributions from both the (commensurate) film and the substrate crystal: the abrupt termination of the lattice leads to crystal truncation rods extending between the bulk Bragg peaks in this direction.[16] In each sample three or more Bragg reflections from the film were sampled. In the film cubic lattice coordinates, these Bragg peaks are indexed (100), (110), and (111). The Bragg peaks, however, did not position exactly at these points, but were displaced along the direction perpendicular to the surface. As mentioned above, all unannealed samples were found to have the same general cubic symmetry but differences were present in the form of strain, or distortion from the cube. The annealed $\alpha$-$FeSi_2$ films are similarly strained if one considers a larger near-cubic unit cell with $a'=2a$. From the scans in $q_\perp$, the precise position of the Bragg peaks was determined. Their average gave the lattice spacing perpendicular to the interface. Table I

TABLE I. Lists of results, atomic plane spacing, and in-plane coherence lengths. The samples used for the structure-factor analysis are listed first. Number 1059 is one sample grown in a two-step 1:1 process. Number 1066 is one of the annealed 1:2 grown samples, with the $\alpha$-$FeSi_2$ structure. The uncertainty of the last significant digit is in parentheses.

| Sample No. | Thickness (Å) | $Fe_xSi$ (CsCl) | $\langle d_{(111)}\rangle$ (Å) | Rhombohedral distortion (%) | In-plane coherence length (Å) |
|---|---|---|---|---|---|
| 7001 | 270 | $x=0.88$ (13) | 1.630 (3) | 3.8 (2) | 2300 |
| 1023 | 105 | $x=0.69$ (8) | 1.540 (6) | −1.8 (4) | 4200 |
| 1059 | 45 | $x=1$[a] | 1.640 (2) | 4.5 (2) | 1100 |
| 1066 | 40 | n.a. ($\alpha$-$FeSi_2$) | 1.523 (16)[b] | −2.5 (10) | 6700 |

[a]From growth conditions
[b]$d$ for (112) of tetrahedral cell.

lists the plane spacing $d$ for two samples used for the structure-factor analysis and other representative samples. No displacement of the peaks parallel to the interface was detected indicating the lattice spacing parallel to the interface is the same as (half) that of the silicon lattice constant. The rhombohedral distortion can be calculated from this by

$$\varepsilon_R = \frac{a_\perp - a_\parallel}{a} ,$$

where $a$ is an estimated bulk lattice constant. The value of $a$ was estimated from $a_\perp$, $a_\parallel$, and the elasticity constant of Possion's ratio $\sigma$ taken to be 0.35, a value determined by earlier Brillouin scattering measurements;[17] this is a very small correction, however. The resulting values for the rhombohedral distortion are plotted in Fig. 4 as a function of film thickness. The drawn lines are only to bring attention to how the samples fall in three classes: compressive strain or positive rhombohedral distortion, and tensile strain or negative rhombohedral distortion for both unannealed and annealed. The tensile-strained films are the ones grown at the 1:2 stoichiometric ratio and the compressive-strained films were grown at the 1:1 ratio. From the strain calculations, the estimated bulk lattice parameter for the 1:1 films is about 2.78 Å, which in close agreement to a theoretical ($T=0$ K) value of 2.72 Å for FeSi (CsCl) in Ref. 18. For the 1:2 disordered unannealed films, the estimated bulk lattice parameter is 2.69 Å.

This difference in strain supports the defect CsCl structure model. As iron vacancies are introduced into the CsCl structure, the average coordination for Si atoms decreases. This generally results in a contraction of the lattice. Such a contraction with the decrease in the Fe stoichiometry would result in the compressive to tensile strain difference as shown for the 1:2 grown films. The opposite would be expected if Si were substituting for the Fe atoms. Silicon in iron sites of the CsCl structure would produce an expansion from the increased coordination of the Si, in contraction to the measured results. As mentioned above, the strain could explain why the determined Fe stoichiometry (from the structure-factor analysis) was different from the expected growth stoichiometry: Large stoichiometry extremes would result in larger extremes in strain. Partial adjustment of the stoichiometry (maybe involving the substrate) to relieve strain would cause the final value to be closer to the (nominal) intermediate value of a completely relaxed film. More experiments are needed to answer this hypothesis and the questions it raises, such as, how stoichiometry and strain are related in these systems.

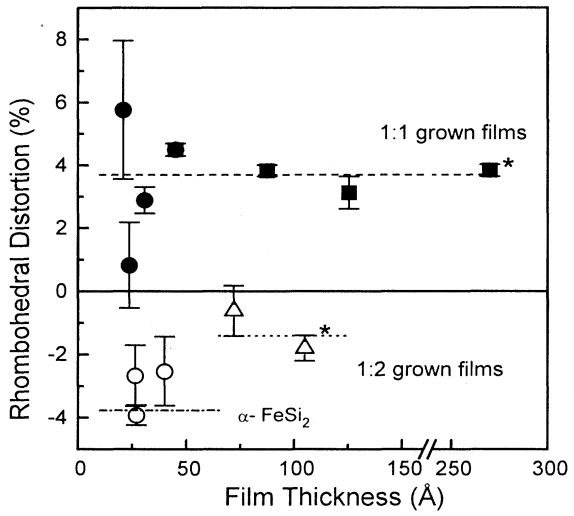


FIG. 4. Rhombohedral distortion of silicide films vs film thickness. The solid squares are for films grown with 1:1 Fe to Si stoichiometry. The solid circles are for the two step 1:1 grown films. The open triangles are unannealed 1:2 grown film. The open circles are for annealed films grown with 1:2 stoichiometry (and found to be $\alpha$-$FeSi_2$). A positive distortion corresponds to compressive strain. The lines are drawn only to aid the eye. The two samples used for the structure-factor analysis are marked with asterisks.

The third set of points on Fig. 4 show that the effect of annealing is apparently to increase the strain in the 1:2 grown films. This is understood to be due to the $c/a$ ratio of 1.9 instead of 2.0, however. These annealed films have a tetragonal structure so they no longer have a simple rhombohedral strain. Taking the bulk $\alpha$-$FeSi_2$ lattice parameters,[19] the near-cubic unit-cell volume is 7.3% smaller than Si, consistent with the $-3.7\%$ linear contraction observed.

## VI. THICKNESS AND UNIFORMITY OF THE FILMS

The $q_\perp$ scans also show thin-film oscillations (Laue fringes) to the sides of the Bragg peaks. A least-squares fit to the oscillations from some of the samples was possible using a theory described in Ref. 20. The theory considers a discrete distribution of film domains with thickness $Nd$. The total scattered amplitude is then the sum of the individual domain amplitudes over this distribution:

$$A = \sum_N P_N F(q) \frac{1-e^{iq_\perp Nd}}{1-e^{iq_\perp d}} .$$

The structure factor $F(q)$ includes the atomic structure of the film and, therefore, the transverse momentum dependence. Assuming a binomial distribution for $P_N$, the sum can be performed analytically. The sum is analogous to the moment generating function for this statistical distribution. A binomial distribution can be justified since it approaches a Gaussian distribution in the continuum limit. Squaring the amplitude gives the intensity function as

$$I = |F(q)|^2 \frac{\frac{1}{4}(1-\alpha)^2 + \alpha \sin^2[\tilde{N}d(q_\perp - \zeta)]}{\sin^2(q_\perp d/2)} ,$$

where we have used the following definitions:

$$\alpha = [1-4\varepsilon(1-\varepsilon)\sin^2(q_\perp d/2)]^{(1/2)\tilde{N}} ,$$

$$\zeta = \frac{1}{d}\arctan\left[\frac{\varepsilon \sin q_\perp d}{\varepsilon \cos q_\perp d + (1-\varepsilon)}\right] ,$$

$$\tilde{N} = M/1-\varepsilon \quad \text{and} \quad \varepsilon = s^2/M .$$

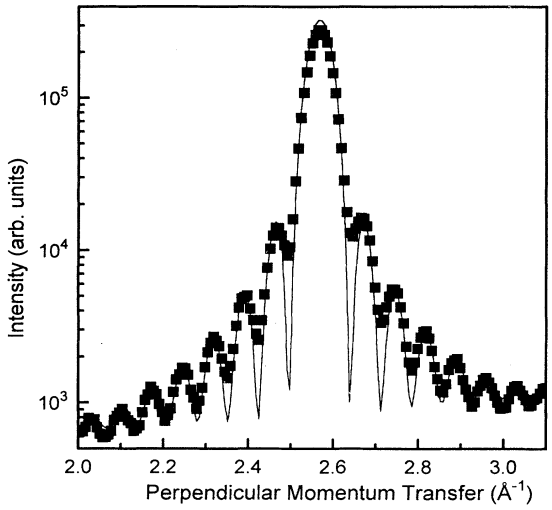


FIG. 5. Example scan of silicide film Bragg peak (110) vs momentum transfer perpendicular to the surface $q_\perp$. The solid curve is a least-squares fit for a thin film of thickness 89 and a roughness of 7 Å.

These quantities relate to physical quantities describing the films: the mean-film thickness in *Md* and the roughness is *sd*. Thus, from the fringe spacing, an accurate determination of thickness is obtained as well as an estimated roughness or variation of the film thickness. An example of the data is given in Fig. 5 where the curve is the best fit for a film thickness of 89 Å and a roughness of 7 Å. The growth conditions indicated a thickness of 70 Å. Some silicide samples had more complicated peak shapes probably due to strain gradients that could not be fit by this simple model.

Table I lists the in-plane coherence length for some of the film samples. Using cross-section scans through the film Bragg peaks along a direction parallel to the interface, the in-plane coherence length was determined from the peak's full width at half maximum (FWHM) by

$$L = 2\pi/\Delta q(\mathrm{FWHM}) .$$

For all samples, the coherence perpendicular to the interface is limited to the thickness of the films, as demonstrated above.

## VII. CONCLUSIONS

We have determined the structure of iron-silicide films grown at room temperature on a Si(111) substrate. The films grow pseudomorphically and commensurate in the (111) plane. The film Bragg-peak positions and the absences of other peaks determine the film structure to be that of the cubic CsCl structure (space group $Pm\bar{3}m$) with about half the unit cell of the Si substrate for all the unannealed samples. The total absence of peaks at the positions of a fcc lattice informs us that there is no $CaF_2$ phase (space group $Fm\bar{3}m$) even for 1:2 stoichiometric samples. The CsCl structure agrees with TEM diffraction and reflection high-energy electron-diffraction (RHEED) experiments.[3,4]

Although unannealed samples show exclusively the symmetry of the CsCl structure, there is a pronounced strain effect as the stoichiometry is varied, as seen in the figure of rhombohedral distortion. The rhombohedral distortion changes sign between the different extremes of stoichiometries. This is correlated with a clear change in structure factors. Unlike the previous TEM and RHEED experiments, our structure-factor measurements allow us to determine the atomic occupation within the lattice. This constitutes the strongest proof so far of a vacancy model with partially occupied Fe sites in the CsCl

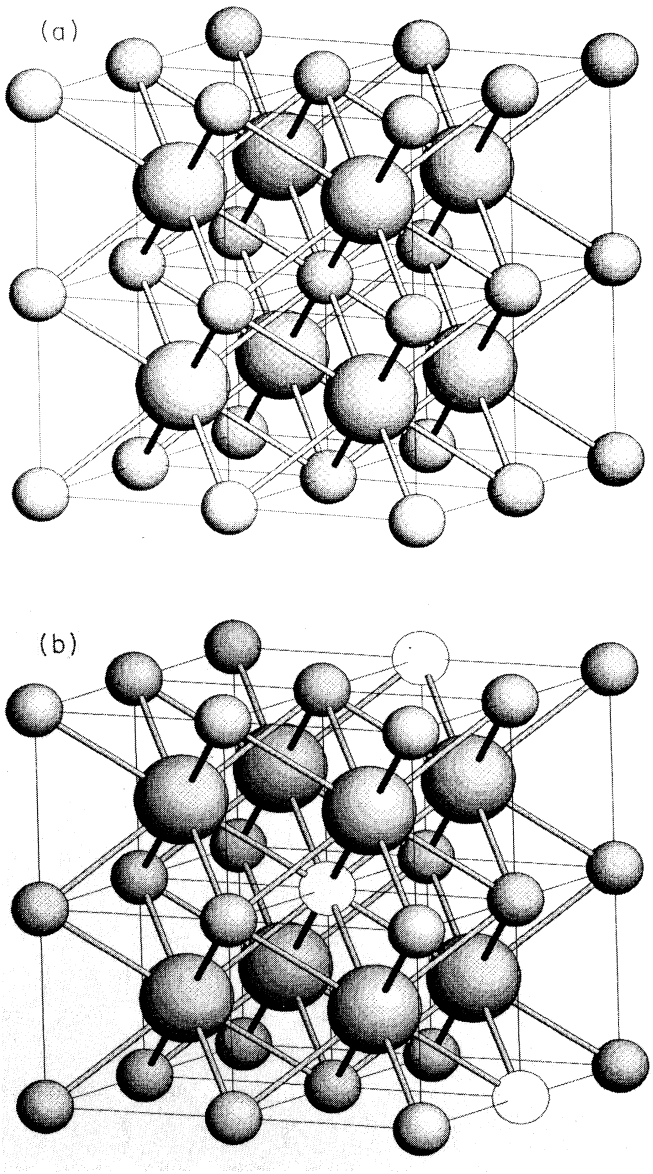


FIG. 6. Lattice representations for (a) FeSi (CsCl structure) and (b) $Fe_x\square_{1-x}Si$ (disordered CsCl structure). The smaller and larger spheres represent Fe and Si atoms, respectively. The open circles in (b) represent disordered Fe vacancies.

structure. Therefore, a better notation for the composition of this silicide would be $Fe_x\square_{1-x}Si$ with $0.5 \leq x \leq 1$ for the fraction of Fe. The iron vacancies are represented by open circles in the disordered CsCl structure in Fig. 6. By randomly removing up to half of the Fe from the CsCl silicide, the average local symmetry is not changed, but change is clearly seen in the comparison between structure factors, and is also consistent with the rhombohedral-distortion data. If the Fe vacancies were in fact ordered at $x = 0.50$, the resulting structure would be the $CaF_2$ structure [Fig. 1(c)]. Although not present in any of our samples, this has been seen with TEM on thin films of 1:2 ratio iron silicide that are annealed slowly and transformed to islands of $\gamma$-$FeSi_2$ ($CaF_2$ structured) phase.[7] This paper's conclusions are consistent with the idea suggested by the TEM experiment, that the as-grown 1:2 stoichiometry films are disordered, but can be come ordered upon annealing.

## ACKNOWLEDGMENTS

We acknowledge the support from the U.S. Department of Energy under Contract No. DEFG02-91ER45439. D.M.S. acknowledges support from Humboldt-Stiftung, Germany. The National Synchrotron Light Source is supported by Department of Energy, Contract No. DEAC012-76CH00016.

[1]C. A. Dimitriades, J. H. Werner, S. Logothetidis, M. Stutzmann, J. Weber, and R. Nesper, J. Appl. Phys. **68**, 1726 (1990); C. Giannini, S. Lagomarsino, F. Scarinci, and P. Castrucci, Phys. Rev. B **45**, 8822 (1992).

[2]N. E. Christensen, Phys. Rev. B **42**, 7148 (1990).

[3]N. Onda, J. Henz, E. Müller, K. A. Mäder, and H. von Kanel, Appl. Surf. Sci. **56-58**, 421 (1992).

[4]H. von Känel, K. A. Mäder, E. Müller, N. Onda, and H. Sirringhaus, Phys. Rev. B **45**, 13 807 (1992).

[5]U. Kafader, C. Pirri, P. Wetzel, and G. Gewinner, Appl. Surf. Sci. **64**, 297 (1993); U. Kafader *et al.*, Europhys. Lett. **22**, 529 (1993).

[6]N. Onda, H. Sirringhaus, S. Goncalves-Conto, C. Schwarz, E. Müller-Gubler, and H. von Känel, in *Evolution of Surface and Thin Film Microstructure,* edited by H. A. Atwater, E. Chason, H. Grabow, and M. Lagally, MRS Symposia Proceedings No. 280 (Materials Research Society, Pittsburgh, 1993), p. 581.

[7]H. Sirringhaus, N. Onda, E. Müller-Gubler, P. Müller, R. Stalder, and H. von Känel, Phys. Rev. B **47**, 10 567 (1993).

[8]O. Kubaschewski, *Iron-Binary Phase Diagrams* (Springer-Verlag, Berlin, 1982).

[9]G. A. Prinz, Phys. Rev. Lett. **54**, 1051 (1985).

[10]J. Chevrier, P. Stocker, Le Thanh Vinh, J. M. Gay, and J. Derrien, Europhys. Lett. **22**, 449 (1993).

[11]M. Sauvage-Simkin, N. Jedrecy, A. Waldhauer, and R. Pinchaux, Physica B **194**, 48 (1994).

[12]J. Derrien, J. Chevrier, Le Thanh Vinh, I. Berbezier, G. Giannini, and S. Lagomarsino, Appl. Surf. Sci. **73**, 90 (1993).

[13]N. Onda, H. Sirringhaus, E. Müller, and H. von Känel, J. Cryst. Growth **127**, 634 (1993).

[14]*International Tables for X-Ray Crystallography,* 2nd ed., edited by C. H. MacGillavry and G. D. Rieck (Reidel, Dordrecht, 1983), Vol. III.

[15]Calculated from Debye temperature given in N. Ashcroft and N. D. Mermin, *Solid State Physics* (Saunders, Philadelphia, 1976).

[16]I. K. Robinson, Phys. Rev. B **33**, 3830 (1986); I. K. Robinson and D. J. Tweet, Rep. Prog. Phys. **55**, 599 (1992).

[17]H. von Känel (unpublished).

[18]K. A. Mäder, H. von Känel, and A. Baldereschi, Phys. Rev. B **48**, 4364 (1993).

[19]$a = 2.69$ and $c = 5.13$ Å; W. B. Pearson, *A Handbook of Lattice Spacings and Structures of Metals and Alloys* (Pergamon, New York, 1967), Vol. 2.

[20]P. F. Miceli, C. J. Palmstrom, and K. W. Moyers, Appl. Phys. Lett. **61**, 2060 (1992); P. F. Miceli, in *Semiconductor Interfaces, Microstructure, and Devices: Properties and Applications,* edited by Z. C. Feng (Hilger, Bristol, 1992).

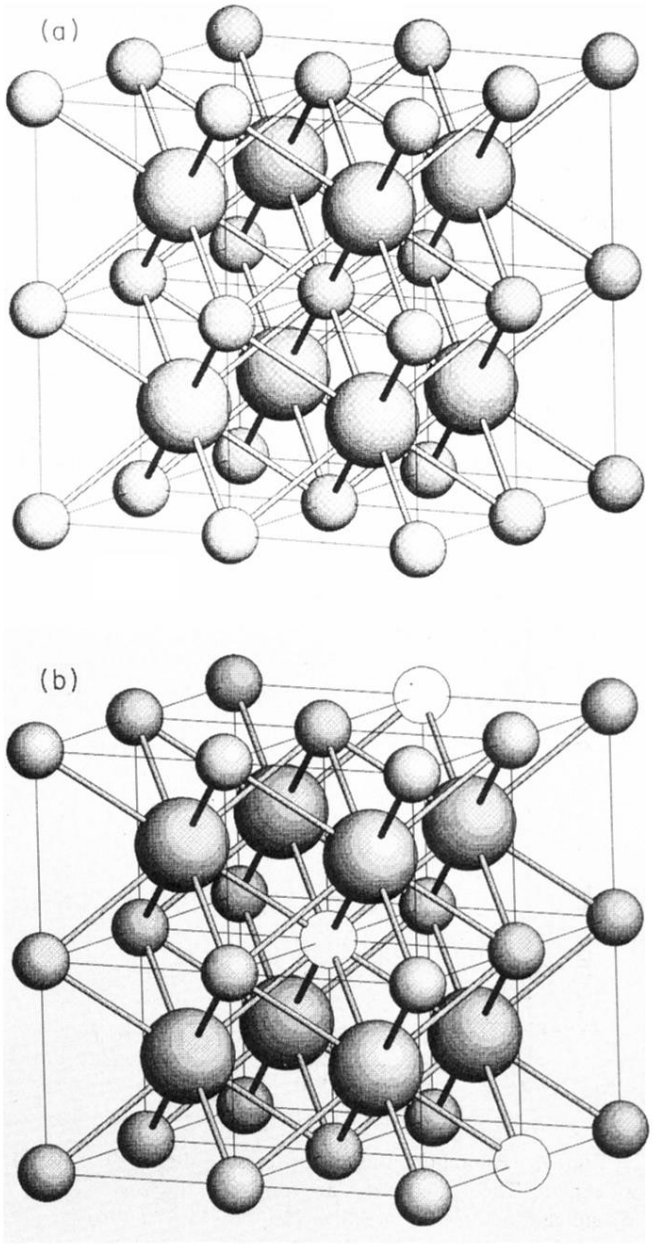


FIG. 6. Lattice representations for (a) FeSi (CsCl structure) and (b) $Fe_x\square_{1-x}Si$ (disordered CsCl structure). The smaller and larger spheres represent Fe and Si atoms, respectively. The open circles in (b) represent disordered Fe vacancies.